Lasers in Manufacturing Conference 2021

Laser process manipulation by axial beam shaping

Joerg Volpp[a,*], Adrien da Silva[a], Alexander Laskin[b]

[a] *Luleå University of Technology, Department of Engineering Sciences and Mathematics, 97451 Luleå, Sweden*
[b] *AdlOptica GmbH, Rudower Chaussee 29, 12489 Berlin, Germany*

Abstract

The laser beam is a highly flexible tool, which is used for many material processing applications. However, new beam shaping technologies open even further possibilities and processing options in order to control the heat input into the material. Beam shaping for high-power applications are usually done by manipulating the spatial intensity distribution in one layer to create e.g. several laser spots, tophat or donut profiles. A new beam shaping device offers the possibility to create up to four focal spots in axial direction, which enables an extended depth of focus (DOF) and thereby tailoring the distribution of the energy along the beam axis. In this work, experiments are shown that present the impact of different axial beam shaping settings on process behaviors during laser material processing. At low processing velocities, the amounts of measured spatters at the bottom side of the processed sheets show a reduced number of spatters compared to higher speeds. It is assumed that a stable keyhole opening is achieved that prevents the spattering.

Keywords: Multi-focus optic, Laser welding, Laser cutting, Melt pool spatter

1. Introduction

Laser material processing is a widely used technology and offers many more possibilities due to its flexibility and controllability. Typical laser material processes use a single beam for e.g. cutting, welding, marking or surface treatment. The spatial laser intensity distribution can vary from being (almost) Gaussian when using single-mode lasers to multi-mode beam profiles, showing donut-like profiles (common for CO_2-lasers) or tophat-profiles (typical for fiber-transferred laser light of solid-state lasers).
Commonly, the laser beam is used as it is produced by the laser machine. However, beam shaping techniques are increasingly demanded since they offer the possibility of more control of the energy transfer from the

* Corresponding author.
E-mail address: jorg.volpp@ltu.se.

laser beam to the material. In laser beam hardening, beam shaping is a well-known technique. E.g. Chen et al., 2005 and Sun et al., 2014 used already lines for increasing the treatable surface area per time. Since the laser output power of laser machines increases during their development, more flexibility is possible for redistributing the intensity of the laser beam.

Another method of beam shaping is laser beam scanning. Qiu and Kujanpää, 2012 used e.g. movable mirrors and Holzer et al., 2017 used beam shaping optics. A comparably small laser spot is thereby moved onto the material surface to locally treat the material. Schultz et al., 2014 showed that laser beam scanning can reduce spattering and increase gap bridgability during laser welding.

However, all commonly used beam shaping techniques aim to adapt the spatial intensity distribution. New beam shaping opportunities open a new parameter for laser process design. Laskin et al., 2018 recently demonstrated that axial beam shaping is possible also for high-power lasers. First tests by Volpp and Vollertsen, 2019 showed already that the partial penetrated keyhole during laser welding can be influenced, while also the spatter formation can be altered. Due to this observation, further tests were conducted and are presented in this work to get a better understanding of the impact of axial beam shaping on material processes.

2. Methods

Laser material processing was conducted using a foXXus optic (Adloptica). The laser beam from an IPG fiber laser was transferred through the processing fiber (fiber diameter 100 µm) to the optics. As collimation optics, the foXXus optics was used having a focal length of 200 mm to the center of the axially shaped beam. The focusing lens had a focal length of 200 mm. The theoretical focal beam diameter was therefore 100 µm. The beam caustic was measured using a Prometec beam measurement devise that records the spatial laser intensity distribution in several layers along the laser beam axis. The recorded axial beam caustics can be seen in Fig. 1. The foXXus optic has three modes, namely two-close (2c), two-distant (2d) and four beam waists denoted by F_n. During the investigation, the relative position between the axial laser position and the material surface were varied.

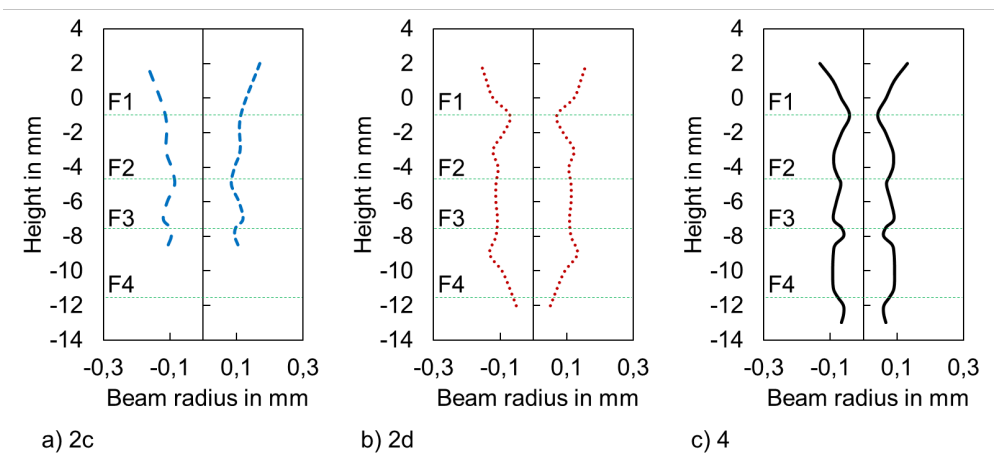

Fig. 1. Measured beam profiles at axial beam shaping with a) two foci close (2c), b) two foci at further distance (2d) and c) four foci (4)

In order to prevent back-reflections into the laser system, the laser beam was angled 20º in trailing direction. The laser output power was kept constant for all experiments at 5 kW. Argon was used as shielding gas, applied at 19 l/min. Two materials were used, namely Aluminum (thickness 4 mm) and Titanium (thickness 1 mm). The laser beam was moved over the specimens at a length of 45 mm. Besides the axial position of the laser beam, the speed and the axial beam shape were varied. Spatter analysis was done using a Matlab routine that detects spatters in each frame of the high-speed-videos as shown by Volpp and Vollertsen, 2016.

3. Results

High reflective aluminum material was tested using different beam shapes (Fig. 2). Both tested beam shapes showed an accumulation of molten material below the processing zone. At 2d-configuration (Fig. 2a), the energy input in the lower melt pool was not sufficient to open the keyhole on the bottom side, while at 4-foci configuration, the lower keyhole opening opened and closed (Fig. 2b).

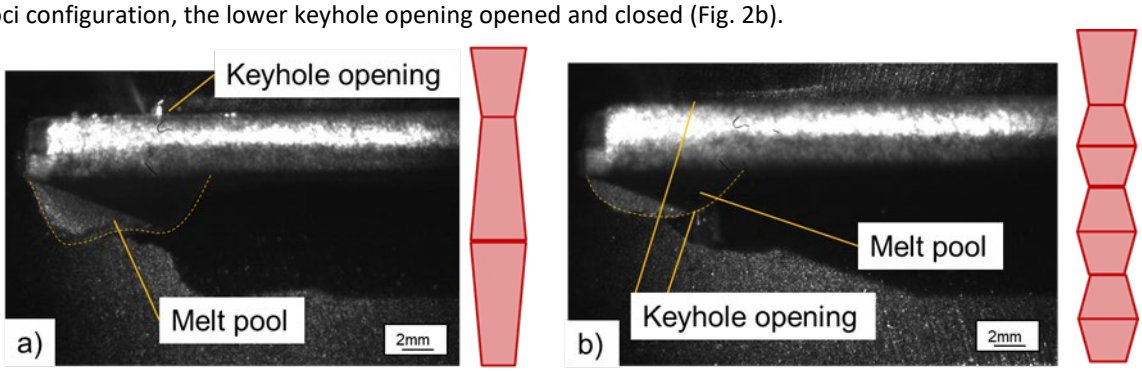

Fig. 2. High-speed-imaging frames of aluminum processing at a) 2d-foci and b) 4-foci arrangement and 0.5 m/min process velocity

When processing titanium at different axial beam shapes (Fig. 3), characteristic differences can be observed. The smallest waist on the material surface (Fig. 3a), resulted in a cutting process with a stable vapor plume above the material and removal of the material. At wider spatial beam shapes (Fig. 3b), the ejection of material is reduced and limited to a few random ejections at a very wide spatial beam shape (Fig. 3c).

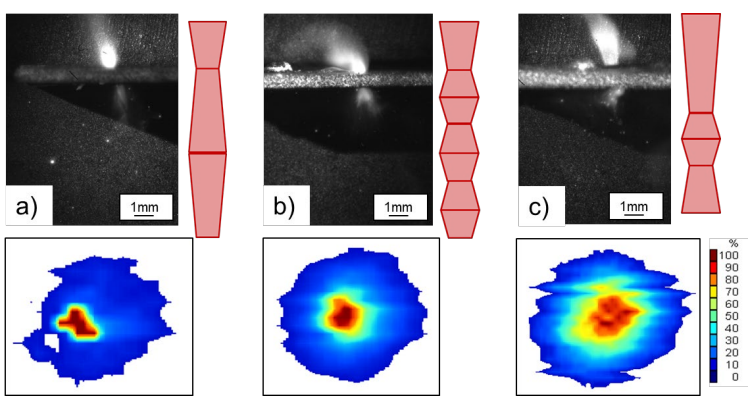

Fig. 3. High-speed-imaging frames and the related beam shape on the material surface at a) 2d-, b) 4-, c) 2c-arrangement and 7.5 m/min process velocity

Titanium processing was done at different processing velocities at 2d-configuration (Fig. 4). Keyholes at all tests penetrated through the whole thickness of the material, but different vapor plumes were observed. As expected, a higher line energy (power per velocity) leads to more evaporation and brighter vapor plume appearance. Below the processing zone, different behaviors of the ejected spatters was observed.

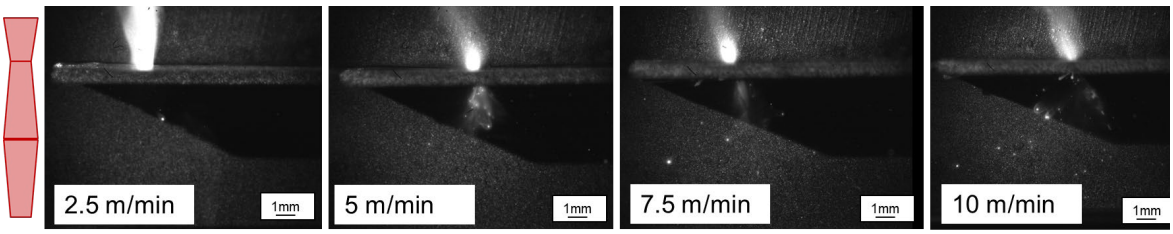

Fig. 4. High-speed-imaging frames of titanium processing at 2d-foci arrangement and varied process velocity

The results of the spatter analysis is shown in Fig. 5. At higher process velocities, the amount of spatters per time increases, while the spatter speed decreases.

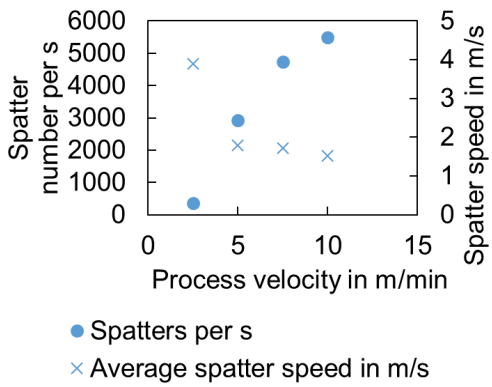

Fig. 5. Spatter analysis at different processing velocities at 2d-foci arrangement of titanium processing (see Figure 4)

4. Discussion

The beam shaping in the foXXus is done based on superpositioning up to four separate beams. Therefore, the created beam waists denote the focal positions of the single beams, while around the main peak, increased intensity values from the other beams can be seen (e.g. Fig. 3). This has to be kept in mind when evaluating the results.

The experiments aimed at analyzing the material processing of thin sheets with enough power that the keyhole can penetrate the whole material thickness.

Although the intensity of the laser beam results in a keyhole formation, the recoil pressure seems not sufficient to push the molten aluminum material out as it is done in remote cutting processes. The melt accumulates below the processing zone. This accumulation leads to an observable opening and closing of the keyhole opening on the bottom side of the processing zone. Due to the oxide layer surrounding the molten aluminum, the material cannot be removed from the processing zone. Only when the keyhole can open to the bottom of the melt pool and locally destroy the oxide layer, small melt pool spatters can be ejected.

The 4-foci axial beam shape configuration seems to lead to a more homogeneous energy distribution on the keyhole wall that enables the partial opening of the keyhole to the bottom at aluminum and titanium processing. However, due to multiple reflections on the keyhole walls as shown by Fabbro et al., 2018, the energy distribution inside the keyhole differs from the measured beam caustic (Fig. 1). Parts of the intensity around the main peak are reflected on the material surface around the keyhole entrance. The increasing beam diameter of the 2d-caustic (Fig. 6a) leads to a fluctuation of the keyhole outlet on the bottom, while the low energy input can eject melt spatters. On the other hand, the intensity around the keyhole can lead to a wider keyhole opening (Fig. 6b,c), which has been shown by Mizutani and Katayama, 2003 to contribute to a higher processing stability. The 4-foci configuration seems to combine the advantages of a superpositioned spatial beam shape on the material surface for providing a wide and stable keyhole opening with the elongation of the beam waist to provide energy into deeper keyhole regions (Fig. 6b). The wide superimposed energy input of the 2c-configuration leads to an increased heat input in the upper keyhole regions and a wide melt pool, while small spatters occur on the bottom side when the keyhole can penetrate through the melt pool and the recoil pressure is sufficient to eject spatter.

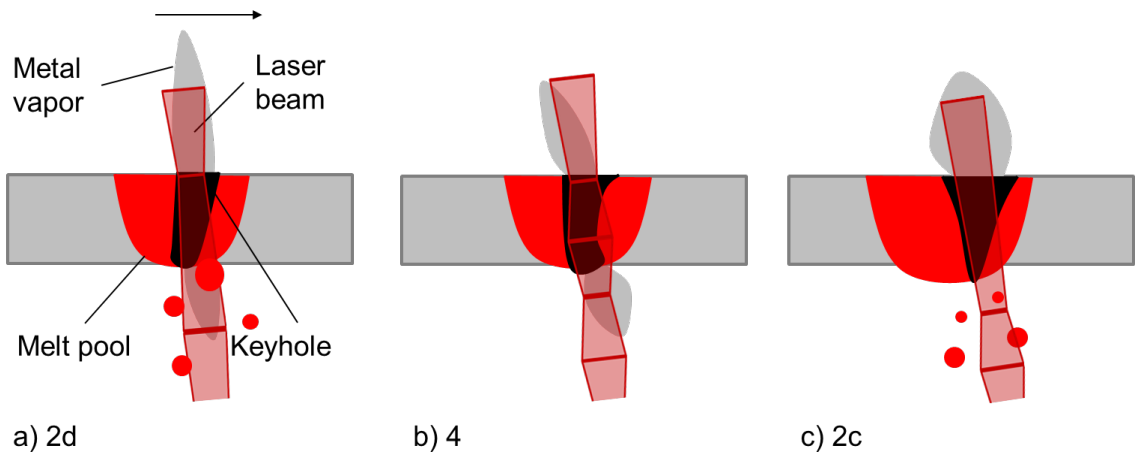

Fig. 6. Schematic of the processing at a) 2d-, b) 4- and c) 2c- configuration

A similar effect is likely to happen also at different processing velocities (Fig. 7). At low velocities, the wide keyhole produces a large vapor plume, while at the same time, the melt pool around the keyhole becomes large as well and the recoil pressure is not able to push material out. At higher velocities, the melt pools are smaller and the high intensity of the laser beam in lower keyhole regions can still produce a high enough recoil pressure to produce vapor and spatter. Since the keyhole is leaning more at higher velocities, the high intensities of the laser beam can act on molten material, while at low velocities the probability of laser rays escaping through the bottom opening is higher.

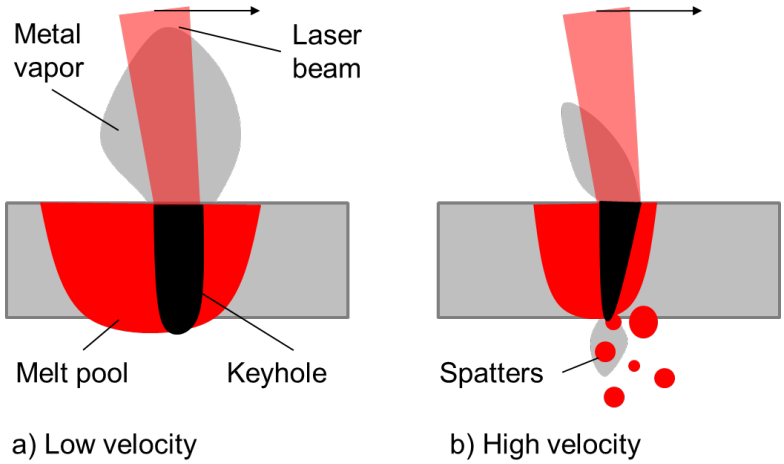

Fig. 7. Schematic of the processing at a) low and b) high process velocity

The experiments show that different axial beam shapes can be used to alter the process behavior of laser material processing.

5. Conclusions

In this paper, a newly developed axial beam shaping optic was used for laser material processing of different material sheets, while high-speed-image observations could show the process behavior and spattering effects. It could be shown that axial beam shaping can alter the energy input into the keyhole, which is indicated by different keyhole vapor and recoil pressure effects on melt pool spattering. Depending on the process needs, the axial beam shaping can support the creation of melt ejection or its avoidance.

Acknowledgements

The authors gratefully acknowledge funding from EIT RawMaterials for the project SAMOA - Sustainable Aluminium additive Manufacturing fOr high performance Applications, no. 18079, from Vinnova - Sweden´s innovation agency for the project SYMAX - Symbiotic redesign by laser-transferred waste metal maxels, no. 2019-02458 and from Vetenskapsrådet for the project SMART – Surface tension of Metals Above vapoRization Temperature, no. 2020-04250.

References

Chen, Y., Gan, C. H., Wang, L. X., Yu, G., & Kaplan, A. (2005). Laser surface modified ductile iron by pulsed Nd: YAG laser beam with two-dimensional array distribution. Applied surface science, 245(1-4), 316-321.

Fabbro, R., Dal, M., Peyre, P., Coste, F., Schneider, M., & Gunenthiram, V. (2018). Analysis and possible estimation of keyhole depths evolution, using laser operating parameters and material properties.

Holzer, M., Zapf, K., Kronberger, S., Henkelmann, F., Mann, V., Hofmann, K., Roth, S., & Schmidt, M. (2017) Influence of dual beam on process stability in laser beam welding. Proceedings of Lasers in Manufacturing Conference 2017 (LiM), Contribution190

Laskin, A., Volpp, J., Laskin, V., & Ostrun, A. (2018, February). Beam shaping of focused radiation of multimode lasers. In High-Power Laser Materials Processing: Applications, Diagnostics, and Systems VII (Vol. 10525, p. 1052507). International Society for Optics and Photonics.

Mizutani, M., & Katayama, S. (2003, October). Keyhole behavior and pressure distribution during laser irradiation on molten metal. In International Congress on Applications of Lasers & Electro-Optics (Vol. 2003, No. 1, p. 1004). Laser Institute of America.

Qiu, F., & Kujanpää, V. (2012). Surface hardening of AISI 4340 steel by laser linear oscillation scanning. Surface engineering, 28(8), 569-575.

Schultz, V., Seefeld, T., & Vollertsen, F. (2014). Gap bridging ability in laser beam welding of thin aluminum sheets. Physics Procedia, 56, 545-553.

Sun, P., Li, S., Yu, G., He, X., Zheng, C., & Ning, W. (2014). Laser surface hardening of 42CrMo cast steel for obtaining a wide and uniform hardened layer by shaped beams. The International Journal of Advanced Manufacturing Technology, 70(5-8), 787-796.

Volpp, J., & Vollertsen, F. (2016). Keyhole stability during laser welding—part I: modeling and evaluation. Production Engineering, 10(4-5), 443-457.

Volpp, J., & Vollertsen, F. (2019). Impact of multi-focus beam shaping on the process stability. Optics & Laser Technology, 112, 278-283.